

1 **GLOBAL ASSESSMENT OF SEAWATER INTRUSION PROBLEMS (STATUS**
2 **AND VULNERABILITY)**

3 LETICIA BAENA RUIZ^(1,*), DAVID PULIDO-VELAZQUEZ⁽²⁾, ANTONIO-JUAN
4 COLLADOS-LARA⁽³⁾, ARIANNA RENAU-PRUÑONOSA⁽⁴⁾, IGNACIO MORELL⁽⁵⁾

5 1. IGME, Granada, Spain. lbaenar@gmail.com

6 2. IGME and UCAM, Granada, Spain. d.pulido@igme.es

7 3. IGME, Granada, Spain. ajcollados@gmail.com

8 4. Jaume I University, Castellón, Spain. arenau@guest.uji.es

9 5. Jaume I University, Castellón, Spain. morell@uji.es

10 * Corresponding author

11 Keywords: global change; seawater intrusion; coastal aquifer; lumped indices;
12 vulnerability

13 **Abstract**

14 In this research paper we propose a novel method to perform an integrated analysis of
15 the status and vulnerability of coastal aquifers to seawater intrusion (SWI). The method
16 is based on a conceptual approach of intrusion that allows to summarised results in a
17 visual way at different spatial scales, moving from steady pictures (corresponding to
18 instantaneous or mean values in a period) including maps and 2D conceptual cross-
19 sections and temporal series of lumped indices. Our aim is to help in the identification
20 of coastal groundwater bodies at risk of not achieving good chemical status according to
21 the Water Framework Directive. The indices are obtained from available information
22 about aquifer geometry and historical monitoring data (chloride concentration and

23 hydraulic head data). This method may be applied even in cases where a reduced
24 number of data are available. It does not require complex modelling and has been
25 implemented in a GIS tool that encourages its use in other cases. Analysis of the
26 evolution of historical time series of these indices can be used to assess resilience and
27 trends with respect to SWI problems. This method can be also useful to compare
28 intrusion problems in different aquifers and temporal periods.

29 **1. INTRODUCTION**

30 Seawater intrusion affects a great number of coastal aquifers all over the world, and this
31 is a problem often due to the intense economic activity in these zones and the
32 consequent exploitation of their groundwater resources. Several authors have
33 highlighted this problem in Africa (Steyl and Dennis 2010; Bouderbala 2015), America
34 (Barlow and Reichard 2010, Boschetti et al. 2015), Asia (Parck et al. 2012; Pratheepa et
35 al. 2015), Oceania (Werner and Gallagher 2006; Werner 2010) and Europe (Custodio
36 2010; García-Menéndez et al. 2016). In Mediterranean Europe, seawater intrusion
37 (SWI) is a common problem in Spain (Guhl et al. 2006; García-Menéndez et al. 2016),
38 Italy (Barrocu 2003; Benini et al. 2016), Greece (Petalas and Lambrakis 2006; Kazakis
39 et al. 2016), and Turkey (Günay 1997; Arslan et al. 2012). It is due to several factors
40 such as a high summer population density and the intensification of irrigated croplands,
41 which increment the risk of SWI. These factors have led to an increasing water demand
42 since the 1970s. Since 2000, after Water Framework Directive (2000) came into effect,
43 there has been an increase in the number of groundwater quality assessment studies, and
44 consequently in the development of methodologies to quantify groundwater pollution in
45 an aquifer.

46 Many different distributed approaches have been applied to assess spatio-temporal
47 distribution of GW quality issues in coastal regions, depending on the aim of the

48 investigation. They can be classified into two main groups: physical quantitative
49 assessment of aquifer status and mixed quantitative-qualitative assessment of
50 vulnerability to seawater intrusion.

51 The spatio-temporal distribution of the aquifer status can be estimated from available
52 information by applying different modelling approaches (simple interpolation methods
53 or sharp interface solutions and density dependent approaches). The flow models have
54 been extensively applied to study SWI problems (Smith 2004; Eeman et al. 2011). They
55 attempt to determine the position of the seawater-freshwater interface and to simulate
56 SWI processes using analytical or numerical procedures. Several authors have discussed
57 the advantages and limitations of different quantitative flow approaches (Llopis and
58 Pulido 2014). Numerical approaches can simulate complex intrusion processes under
59 transient conditions, but they require numerical approaches and excessive data to obtain
60 a parsimonious approach with enough data to calculate representative parameters on a
61 large scale (with significantly greater requirements in density-dependent flow
62 approaches) (Wriedt and Bouraoui 2009).

63 On the other hand, qualitative methods can be applied to assess vulnerability and/or risk
64 mapping in coastal regions. They aim to identify the parts of a groundwater body that
65 could be contaminated as a result of human activities, taking into account physiographic
66 characteristics such as geology or piezometric level. A numerical index or score is
67 assigned to the different attributes, which are then weighted. The numerical scores
68 cluster similar areas into classes of vulnerability (e.g., low, moderate and high), which
69 are then displayed on a map. They can be used to define hydrogeological subregions
70 with different levels of severity (Kumar et al. 2015). Due to their easy implementation,
71 many index-based techniques have been applied to assess vulnerability. Several authors
72 have criticised the roughness of these index-based methods, however they also reveal

73 the easy implementation and interpretation of these techniques to get a preliminary
74 assessment of vulnerability of groundwater bodies (Werner et al. 2012).

75 The groundwater vulnerability assessment technique was started in 1987 by Aller et al.
76 (1987) through the development of DRASTIC, though this system has undergone
77 several modifications over time (Kumar et al. 2015). Several indices have been
78 developed to assess vulnerability to pollution (SINTAC (Civita 1994), EPIK (Doerfliger
79 et al. 1999) and AVI (Stempvoort et al. 1993)) but they are not usually employed to
80 evaluate vulnerability to SWI. The GALDIT method was developed by Chachadi and
81 Lobo-Ferreira (2001) with the aim of assessing the spatial vulnerability of
82 hydrogeological settings to SWI. GALDIT has been mostly used to perform large-scale
83 assessments of SWI (Benini et al. 2016). The major drawback of this method is that the
84 effect of pumping on the SWI process is not considered (Trabelsi et al. 2016). Despite
85 this limitation, this model shows many advantages, such as its low computational cost.
86 Moreover, it requires few, easy to collect historical variables and parameters, and it can
87 be applied over large areas. However, vulnerability methods only highlight specific
88 areas in the aquifer that are at risk or prone to pollution due to their intrinsic
89 characteristics, whereas it might be interesting to adopt measures in order to improve
90 them. In the literature, there are examples of works developed to provide a global
91 assessment of aquifer status (e.g., Ballesteros et al. 2016), but none that address aquifer
92 vulnerability.

93 In this paper we propose a new systematic method to analyse status and vulnerability to
94 SWI at different spatial scales. The method is based on a conceptual approach that
95 allows to define steady pictures (representing instantaneous or mean values in a period)
96 to move from maps to 2D schematic cross sections, and temporal series of lumped
97 indices. The analysis of these temporal series of the indices, which summarize global

98 status and vulnerability, allows to study the SWI dynamic, resilience and trend. The
99 proposed method can be useful to identify aquifers in risk of not achieve the objective
100 defined in the Water Framework Directive (2000). The paper is structured as follows.
101 Section 2 describes the method, defining the proposed indices and specifying the steps
102 to obtain them. Section 3 describes the case studies and the available data, while section
103 4 outlines the results and discussion. Section 5 gives our main conclusions.

104 **2. METHODOLOGY**

105 The inputs required and the steps to be followed to apply the method are represented in
106 Figure 1.

107 The **inputs** include variables (to characterise the historical evolution of hydraulic head
108 and chloride concentration) and parameters (to define aquifer geometry and
109 hydrodynamic behaviour) to determine the overall status of the aquifer. The data
110 describing the historical evolution could come from direct observation (monitoring
111 network) or other techniques (geophysical applications, etc.). For the vulnerability
112 assessment, other intrinsic information is also needed as inputs to apply the proposed
113 method.

114 The steps proposed in order to summarize status and vulnerability to SWI through
115 visual pictures and time series are described in the next subsections.

116

117 **Fig 1** Flow chart of methodology

118 **2.1. Assessment of seawater intrusion (SWI) status**

119 The described inputs will be employed to assess SWI status according to the following
120 steps:

121 2.1.1. Maps of chloride concentration

122 Fields (maps) of chloride concentration and hydraulic head can be obtained by applying
123 simple interpolation techniques in each date with enough available information. 3D
124 maps of the saturated thickness (with a finite number of cells) can be obtained by
125 combining hydraulic head maps with the geometry and the storage coefficient. Vertical
126 aquifer geometry and storage coefficient can be obtained from previous 3D models and
127 hydrogeological studies respectively.

128 If there is insufficient information to assess the vertical distribution of chloride
129 concentration, an invariant concentration with depth is assumed at each point, thus
130 obtaining 2D fields of chloride concentration.

131 From chloride concentration and saturated thickness maps, we can define the affected
132 and non-affected zone (areas where the chloride concentration level is above the natural
133 background level). This threshold, which depends on the geochemistry of the aquifer, is
134 difficult to determine. Some European projects (“BRIDGE”) (Dahlstrom and Müller
135 2006) have provided recommendations for its calculation, based on methodologies
136 applied in some countries. Some of them determine the background level as the
137 concentration in non-contaminated areas. Other define the threshold as 90 percentile of
138 the concentration measured in the groundwater monitoring network, while sometimes
139 they only use data from monitoring networks to define a background concentration. In
140 other cases the threshold is based on the typical background level, the origin of the
141 chloride (natural or anthropogenic) and the possible impacts on ecosystems or human
142 health. For this area we can calculate the affected volume taking into account the
143 storage coefficient and the aquifer geometry.

144 2.1.2. 2D cross-sections: Penetration and Thickness. Increment in concentration

145 2D representative cross-sections can be deduced to summarise the mean geometry
 146 (thickness and penetration) and intensity of the intrusion (increment in concentration).
 147 The average affected thickness (T_{ha}) and inland penetration (P) of intrusion can be
 148 calculated as follow:

$$149 \quad T_{ha}(m) = \frac{\sum V_{i(>V_r)}}{\sum S_{i(>V_r)}} \quad (1)$$

$$150 \quad P(m) = \frac{\sum V_{i(>V_r)}}{T_{ha} * L_{coast}} \quad (2)$$

$$151 \quad V_{i(>V_r)}(m^3) = S_i(m^2) * b_i(m) * \alpha \quad (3)$$

152 where:

- 153 - $V_{i(>V_r)}$ is the storage in each cell (m^3) with a concentration greater than V_r ;
- 154 - S_i is the surface area of each cell (m^2);
- 155 - b_i is the saturated thickness at each instant considered (m);
- 156 - α is the storage coefficient;
- 157 - L_{coast} is the length of coastline (m);

158 The chloride concentration (C) of the affected area is:

$$159 \quad C \left(\frac{mg}{l} \right) = \frac{\sum (C_{i(>V_r)} * V_{i(>V_r)})}{V_{(>V_r)}} \quad (4)$$

$$160 \quad V_r \left(\frac{mg}{l} \right) = \text{Reference threshold} \quad (5)$$

161 where:

- 162 - C_i is the concentration (mg/l) in each cell;
- 163 - $V_{(>V_r)}$ is the total storage (m^3) with a concentration greater than V_r ;

164 The increment of concentration (IC) above the threshold (V_r) in the affected volume is:

165
$$IC\left(\frac{mg}{l}\right) = C - V_r \quad (6)$$

166 Cross sections give an overview of the magnitude and intensity of the intrusion process
167 per linear metre of coast at a specific time. Mean cross sections can also be obtained for
168 a time period.

169 2.1.3. Global index: Mass of affected area (Ma)

170 The index Ma is defined as the total additional mass of chloride that causes the
171 concentration in some areas to exceed the natural threshold. It is obtained multiplying
172 the increment of concentration (IC) by Penetration (P) and affected Thickness (T_{ha})
173 from equations 1 and 2.

174
$$Ma\left(\frac{kg}{m}\right) = P(m) * IC\left(\frac{mg}{l}\right) * 10^{-3} * T_{ha}(m) \quad (7)$$

175 The concept of Ma involves some simplifications, which are schematised in Figure 1.

176 While 2D maps and cross sections summarize the extent and magnitude of SWI in an
177 aquifer at a specific time, Ma index show the intensity and temporal evolution of the
178 problem.

179 2.1.4. Resilience and Trend (MART)

180 The evolution of the Ma index can give an overall assessment of the resilience (R) and
181 trend (T) of the aquifer status according to the SWI problem.

182 We propose calculating Resilience as the maximum relative change of the Ma index
183 (relative difference between maximum and minimum value) over six-year periods,
184 which is the horizon defined to update management plans in the Water Framework
185 Directive (2000). Thus, Resilience shows the potential change for a short-term period,
186 taking into account the measures occurred in this period.

187 Trend is also calculated for six-year periods. It is defined as the relative difference
188 between the values of Ma at the beginning and end of the period. A positive trend
189 indicates the mass of water affected is increasing, while a negative trend indicates an
190 improvement in aquifer status.

191 The combination of Mass of affected water body (Ma), Resilience (R) of the water body
192 and Trend (T) of SWI defines the MART index, which summarize SWI evolution in the
193 aquifer.

194 **2.2. Assessment of vulnerability to SWI**

195 While SWI status is calculated using only physical variables (chloride concentration and
196 hydraulic head), vulnerability employs weighted qualitative characteristics. In this
197 study, we summarise vulnerability status based on the application of the GALDIT
198 method (Aquifer type; aquifer hydraulic conductivity; height of groundwater head
199 above sea level; distance from the shore; impact of existing status of SWI; thickness of
200 aquifer being mapped) (Chachadi and Lobo-Ferreira 2005).

201 2.2.1. Maps of vulnerability

202 Vulnerability maps are displayed from GALDIT method. The GALDIT Index is
203 obtained by applying the expression:

$$204 \quad \text{GALDIT Index} = \frac{\sum_{i=1}^6 W_i \cdot R_i}{\sum_{i=1}^6 W_i} \quad (8)$$

205 where W_i is the weight of the i^{th} indicator and R_i is the importance rating of the i^{th}
206 indicator. The GALDIT scores are then classified into three **vulnerability classes**: High
207 (GALDIT Index range ≥ 7.5), Moderate (between 5 and 7.5) and Low (< 5). These
208 vulnerability classes are the threshold to define the “affected zone” (area where

209 vulnerability is higher than the adopted reference threshold (moderate or high
210 vulnerability)).

211 For this area we can calculate the affected volume taking into account the storage
212 coefficient and the aquifer geometry.

213 2.2.2. 2D cross-sections: Penetration and Thickness. Vulnerability classes

214 2D cross sections can be deduced to summarise the mean geometry and intensity of the
215 GALDIT vulnerability score. Penetration (P_{L_GALDIT}) and Thickness ($T_{ha_L_GALDIT}$) can
216 be calculated from formulas 9 and 10:

$$217 \quad T_{ha_L_GALDIT}(m) = \frac{\sum V_{i(>V_r\ GALDIT)}}{\sum S_{i(>V_r\ GALDIT)}} \quad (9)$$

$$218 \quad P_{L_GALDIT}(m) = \frac{\sum V_{i(>V_r\ GALDIT)}}{T_{ha_L_GALDIT} * L_{coast}} \quad (10)$$

$$219 \quad V_{i(>V_r\ GALDIT)}(m^3) = S_i(m^2) * b_i(m) * \alpha \quad (11)$$

$$220 \quad V_r\ GALDIT = GALDIT\ threshold\ (G \geq 7,5; G \geq 5) \quad (12)$$

221 where:

- 222 - $V_{i(>V_r\ GALDIT)}$ the storage in each cell (m^3) with a concentration greater than V_r
223 GALDIT;
- 224 - S_i is the surface area of each cell (m^2);
- 225 - b_i is the saturated thickness at each instant considered (m);
- 226 - α is the storage coefficient;
- 227 - L_{coast} is the length of coastline (m).

228 The intensity of vulnerability is the GALDIT score in each zone for the thresholds
229 established.

230 2.2.3. Global index: L_GALDIT

231 A lumped global value of GALDIT (L_GALDIT) is defined by weighting the GALDIT
232 score for each point with the storage (Equation 13). This weighted value of GALDIT
233 assesses the overall vulnerability of the aquifer. On the other hand, a lumped affected
234 value of GALDIT can be obtained for the different thresholds (Equations 14 and 15).

235
$$L_GALDIT = \frac{\sum(G_i * V_i)}{V} \quad (13)$$

236
$$L_GALDIT_{high} = \frac{\sum(G_{i(\geq 7,5)} * V_{i(\geq 7,5)})}{V_{(\geq 7,5)}} \quad (14)$$

237
$$L_GALDIT_{high+moderate} = \frac{\sum(G_{i(\geq 5)} * V_{i(\geq 5)})}{V_{(\geq 5)}} \quad (15)$$

238 where:

- 239 - G_i is the value of GALDIT in each cell;
- 240 - V_i is the storage in each cell;
- 241 - V is the total storage in the aquifer;
- 242 - $G_{i(\geq 7,5)}$ is the value of GALDIT of each cell greater or equal to 7,5;
- 243 - $G_{i(\geq 5)}$ is the value of GALDIT of each cell greater or equal to 5;
- 244 - $V_{i(\geq 7,5)}$ is the volume of each cell with a value of GALDIT $\geq 7,5$;
- 245 - $V_{i(\geq 5)}$ is the volume of each cell with a value of GALDIT ≥ 5 ;
- 246 - $V_{(\geq 7,5)}$ is the total volume with a value of GALDIT $\geq 7,5$;
- 247 - $V_{(\geq 5)}$ is the total volume with a value of GALDIT ≥ 5 ;

248 2.2.4. Resilience and Trend

249 An analogous procedure to the one described for the MART index is applied to
250 determine the evolution over time of the L_GALDIT index, the Resilience and Trend of
251 aquifer vulnerability.

252 The method employs the spatial distribution of the storage coefficient to obtain affected
253 volume in the lumped indices (MART and L_GALDIT) and hydrogeological
254 parameters as the transmissivity are implicitly considered in the spatial distribution of
255 the hydraulic head, which considers effects of the aquifer system. Even so it does not
256 require complex modelling approaches and has been implemented in a **GIS tool** that
257 encourages its application to other cases.

258 **3. STUDY AREA**

259 **3.1. Geological and hydrogeological characterisation**

260 The study area is situated on the Mediterranean coast of Spain, in Castellon province.
261 Two different aquifers were studied: the Plana de Oropesa-Torreblanca and Plana de
262 Vinaroz (Figure 2). The increasing population since 1970 and the continuing
263 agricultural exploitation have produced SWI problems of different entity in these
264 aquifers.

265 **Fig 2** Situation of the study area and hydrogeology

266 Both aquifers are unconfined, heterogeneous, detrital and multilayer aquifers composed
267 of gravel and sand levels in a silty clay matrix (Ballesteros et al. 2016). Figure 2 also
268 shows the hydrogeology of these aquifers. The transmissivity in the Plio-Quaternary
269 Plana de Oropesa Torreblanca aquifer ranges from 300-1000 m²/day (García-Menéndez
270 et al. 2016) and the storage coefficient varies between 2-12%, while in Plana de Vinaroz
271 these parameters take the value of 250-1200 m²/day and 5-15% respectively.

272 **3.2. Data**

273 Historic data for the variables of chloride concentration and hydraulic head were
274 provided by the Confederación Hidrográfica del Júcar. There are no data for this study

275 area from 1988 to 1989 or from 2001 to 2005. The number of observation wells varies
276 over time and also from one aquifer to another. The number of monitoring points of
277 chloride concentration in Plana de Oropesa-Torreblanca and Plana de Vinaroz aquifers
278 varies between 12-34 and 9-58 respectively, while the monitoring points of hydraulic
279 head ranges between 9-19 and 6-28 in both aquifers.

280 The number of data available was also variable for each observation point over the
281 period. Observation points were considered if they had data for at least 20% of the study
282 period.

283 The chloride concentration exceed 1000 mg/l in zones close to the coast in both
284 aquifers. Points inland exhibit lower concentrations that are more stable through time.
285 Concentrations increased over the 1980s as a consequence of the expansion in irrigated
286 croplands, associated with a period of scarce rainfall. Subsequently, there was a drop in
287 mean chloride concentrations due to the reduction in pumping, together with improved
288 hydrological planning (Figure 3).

289 **Fig 3** Observation points for chloride concentration and evolution of the chloride
290 concentrations in monitoring points in Plana de Oropesa-Torreblanca (top) and Plana de
291 Vinaroz (down) aquifers

292 Groundwater flow in both aquifers approximately follows a NW-SE direction before
293 discharging to the sea. The range of piezometric levels varies significantly depending on
294 the aquifer: in the Plana de Oropesa-Torreblanca the piezometric level at points furthest
295 from the coast is about 3 m a.s.l., while in the Plana de Vinaroz it reaches 50 m a.s.l.
296 The piezometric level is depressed in both aquifers at certain times in zones close to the
297 coast.

298 Aquifer geometry is derived from previous 3D models (Renau Pruñonosa 2013). The
299 Plana de Oropesa-Torreblanca aquifer is wedge-shaped being the maximum thickest
300 located near to the coastline, where it can reach 90 m thick. The Plana de Vinaroz has a
301 lenticular geometry and its thickness varies between 30 m and 160 m in the inland
302 zones.

303 **4. RESULTS**

304 Here we present the results obtained when the proposed methodology was applied to the
305 two case studies.

306 **4.1. MART Index**

307 4.1.1. 2D – 3D maps. Evolution of chloride concentration and affected volume
308 (Graphics)

309 In terms of the natural background, two different chloride thresholds were used for the
310 calculations. First, a chloride concentration level is established according to the natural
311 background for each aquifer. In CHJ (2016) a reference value of 1100 mg/l is
312 established for both Plana de Oropesa-Torreblanca and Plana de Vinaroz aquifers. In
313 order to analyse the sensitivity to the threshold value, we also tested a threshold of 250
314 mg/l, which is the default value for all aquifers set in other previous studies (Ballesteros
315 et al. 2016).

316 Figure 4 shows an example of the chloride concentration map obtained, with the
317 affected and unaffected zones for both thresholds.

318 **Fig 4** Chloride concentration maps in Plana de Oropesa-Torreblanca for October 1985

319 The 2D maps of chloride concentration show that the zone of SWI in Plana de Oropesa-
320 Torreblanca aquifer grew. However Plana de Vinaroz aquifer has undergone a slight

321 improvement in the study period. Moreover the affected zone in the Plana de Oropesa is
322 significantly greater than for Plana de Vinaroz (Figure 5a).

323 The mean concentration in the zone affected for each aquifer, based on the natural
324 background threshold concentration, lies between 2000-2500 mg/l in both aquifers over
325 almost the entire period (Figure 5b). Although a fall in mean chloride concentration of
326 the affected zone is observed in Plana de Oropesa-Torreblanca aquifer from 1977 to
327 1983, it does not indicate an improvement in the water quality in this period since the
328 affected volume increased in this period (Figure 5a). Chloride concentration is spread
329 over a wider area although the mean concentration in the impacted zone diminished.

330 **Fig 5** Evolution of (a) affected volume (rg (%)) and (b) average chloride concentration
331 in total aquifer and in the affected volume for the two aquifers

332 The mean chloride concentration in the entire aquifer shows an increasing trend until
333 1987 (Figure 5b), which may be explained by the increased abstractions made during
334 this period; after this date, chloride concentrations fell again. The greater the distance
335 between the mean aquifer concentration and the mean concentration in the affected
336 zone, the better the overall status of the aquifer. This does not mean that the aquifer
337 does not suffer grave SWI problems in certain zones. In the Plana de Oropesa-
338 Torreblanca these curves are very close, and so there are significant SWI problems over
339 almost all of the aquifer, the difference being much greater than in the Plana de Vinaroz.

340 Lastly, we analysed the sensitivity of the results to variations in the reference value
341 used. The volume affected using a threshold of 250 mg/l for the two aquifers is much
342 greater than when using a threshold corresponding to the natural background of each
343 aquifer (Figure 5a). In contrast, of course, the mean concentration of the zone affected
344 using the natural background threshold (Figure 5b) is much larger. This phenomenon

345 highlights the need to determine the natural background of each aquifer precisely, since
346 the assessment of whether there are SWI problems is quite sensitive to this threshold
347 value.

348 4.1.2. 2D cross-sections: Penetration and Thickness. Increase in concentration

349 **Fig 6** Average cross-sections for two thresholds (natural background and 250 mg/l)
350 (MART index) over the period 1977-2015 (vertical exaggeration scale: 500)

351 The volume of the Plana de Vinaroz aquifer is significantly larger than the Plana de
352 Oropesa-Torreblanca (Figure 6). In both aquifers, the thickness affected is greater than
353 the mean thickness of the aquifer. These results are consistent with the aquifer geometry
354 and the location of affected areas.

355 Again, the sensitivity of the results to the reference value used can be seen. The lower
356 the value of the threshold, the further the affected zone extends inland. For example,
357 using the 250 mg/l threshold, the entire Plana de Oropesa-Torreblanca aquifer is
358 affected during certain years.

359 Both penetration and thickness reveal the proportion of the aquifer affected.

360 4.1.3. Global index: Mass of affected area (Ma)

361 **Fig 7** Evolution of the global index, Ma, in the two aquifers studied

362 The trend of the index Ma in the two aquifers is similar for both thresholds tested
363 (Figure 7). In general, there was a period when the water quality in the aquifers fell
364 continuously (1977-1986), with Ma rising until 1986. In subsequent years, there was a
365 generalised improvement in both aquifers, particularly after 2007. This improvement
366 could be the result of the wet period from 2002 to 2004 (García-Menéndez et al. 2016)

367 and the effect of newly implemented policies to comply with the Water Framework
368 Directive (2000).

369 The value of Ma (Figure 7) in the Plana de Oropesa-Torreblanca for the natural
370 background is greater than in the Plana de Vinaroz, indicating that the Plana de
371 Oropesa-Torreblanca is in a more critical state than the Plana de Vinaroz. This index,
372 Ma, provides information about the overall importance of SWI in each aquifer and its
373 evolution over time. For a more detailed description of the problem, this index can be
374 combined with the mean concentration of the affected zone (to give an idea of the
375 intensity of the problem) and the 2D section (which informs about the size of the zone
376 affected). For example, comparing the mean concentration of the affected zone when
377 considering the natural background level as the threshold for identifying the presence of
378 SWI in each of the two aquifers (Figure 5b), it can be seen that they take similar values
379 (2000–2500 mg/l); however, the section affected in the Plana de Oropesa-Torreblanca
380 (Figure 6) and the proportion of its volume affected (Figure 5a) are much greater than in
381 the Plana de Vinaroz. These results indicate that the Plana de Oropesa-Torreblanca
382 aquifer suffers grave problems due to SWI over almost all its entirety.

383 4.1.4. Resilience and Trend (MART)

384 Higher values of Resilience were obtained for the period up to 1987 (Figure 8), which
385 indicates that changes in the intrusion were more significant. The value of Trend in the
386 Plana de Oropesa-Torreblanca is positive and also elevated, showing that the change has
387 been a deterioration in the state of the aquifer; while in the Plana de Vinaroz there are
388 periods of improvement (negative trend) though the changes are not significant (low
389 resilience values).

390 Although changes have decreased in the last period, the values of Resilience in Plana de
391 Oropesa-Torreblanca aquifer are higher than in Plana de Vinaroz aquifer.

392 The results are represented only for the threshold established by the natural background
393 (1100 mg/l).

394 Due to the geometry and hydrodynamics of each aquifer, it is more complicated in some
395 aquifers to recover good water quality than in others. In this way, the geometry is more
396 of an obstructing factor in the case of Plana de Oropesa-Torreblanca, which is thickest
397 close to the coastline.

398 **Fig 8** Ma, Resilience and Trend in Plana de Oropesa-Torreblanca and Plana de Vinaroz
399 aquifers (scale exaggeration Resilience and Trend: 10000)

400 **4.2. GALDIT Index**

401 4.2.1. Maps. Vulnerability and identification of affected volume (Graphics)

402 Figure 9 shows examples of vulnerability maps from GALDIT for a specific date in
403 both aquifers studied. The red circles indicate zones where changes occurred during the
404 study period (1977-2015).

405 **Fig 9** L_GALDIT maps in Plana de Oropesa-Torreblanca for April 2015

406 This leads to several conclusions. In the Plana de Vinaroz aquifer the zone of mean
407 vulnerability occupies almost the whole aquifer while the zone of low vulnerability is
408 very small since conductivity is greatly elevated in almost the entire aquifer.

409 The Plana de Oropesa-Torreblanca aquifer is highly vulnerable due to the characteristics
410 of its formation (it is an aquifer lying parallel to the coast with a wedge shaped
411 geometry, very shallow inland, thicker close to the coastline, and with high
412 conductivity) and to the elevated chloride concentration along the coastline.

413 Furthermore, the concentration of bicarbonates is low, which is an indicator of the
414 presence of seawater (Chachadi and Lobo-Ferreira 2005).

415 The volume affected when considering each vulnerability threshold shows little
416 temporal variability over the period of study (1977-2015).

417 4.2.2. 2D cross sections: Penetration and Thickness. Vulnerability classes

418 There are certain similarities in the cross-sections of L_GALDIT (Figure 10) and
419 MART. In the Plana de Oropesa-Torrebanca aquifer, the sections obtained for MART
420 for both threshold are similar as those obtained for GALDIT though less so for the
421 Plana de Vinaroz.

422 **Fig 10** Average cross-sections in two aquifers (L_GALDIT index) for the period 1977-
423 2015 (vertical exaggeration scale: 500)

424 It should be borne in mind that the vulnerability and the overall state of the aquifer do
425 not have to concur. Poor quality is not necessarily found in a vulnerable zone. The zone
426 affected by intrusion can be small, even if a large part of the aquifer is classed as
427 vulnerable due to its intrinsic characteristics.

428 4.2.3. Lumped Index: L_GALDIT. Resilience and Trend

429 The aggregated index, L_GALDIT (Figure 11), exhibits little variability compared to
430 the Ma Index (Figure 8). This is due to the various factors that are used in calculating
431 vulnerability (Benini et al. 2016), especially those factors that have greater weight and
432 less spatial variability (conductivity and distance from the coast), which help to smooth
433 out the results.

434 Almost the entire extension of both aquifers has moderate+high vulnerability.
435 Nevertheless, in the Plana de Oropesa-Torreblanca, the mean vulnerability is higher.

436 These results indicate that the Plana de Oropesa-Torreblanca aquifer is much more
437 vulnerable quantitatively, and second, that the vulnerable zone occupies a much larger
438 extension.

439 **Fig 11** L_GALDIT, Resilience and Trend in Plana de Oropesa-Torreblanca and Plana
440 de Vinaroz aquifers (scale exaggeration Resilience and Trend: 100)

441 Resilience and Trend are represented only for the threshold delimiting high
442 vulnerability (GALDIT=7.5). The Resilience values are low and very similar in both the
443 Plana de Vinaroz and Plana de Oropesa-Torreblanca (values less than 0.01). Such low
444 values are due to the fact that the values of the index L_GALDIT vary within a narrow
445 range, as well as to the fact that the index has low variability due to the reasons
446 commented above.

447 **5. CONCLUSIONS**

448 This paper presents a novel methodology for assessing the overall status of seawater
449 intrusion and vulnerability in coastal aquifers using a mixed lumped-distributed
450 analysis. The problem of chloride contamination is represented in coastal aquifers on
451 different spatial scales, obtaining 2D maps, mean cross-sections and an aggregated
452 index of overall state. In addition, we propose an aggregated index for assessing
453 vulnerability, L_GALDIT, based on the GALDIT method that is already known. The
454 method allows the significance of intrusion and vulnerability to be compared across
455 different aquifers and time periods. Moreover, it can be used to assess resilience and
456 trend respect to SWI.

457 In terms of the overall status of the two aquifers studied, we deduce that the Plana de
458 Oropesa-Torreblanca aquifer has a worse state and it needs more important changes in
459 groundwater use. Resilience indicates that this aquifer has more potential to recover a

460 good status, although it would require great changes in the current pumping
461 management. In addition, due to its intrinsic characteristics it has a high vulnerability
462 and is susceptible to contamination.

463 With respect to vulnerability, again the Plana de Oropesa-Torreblanca is the more
464 vulnerable of the two aquifers, both in terms of its extent and magnitude. Though the
465 Plana de Vinaroz is also vulnerable over almost all of its extent, the value for
466 vulnerability is moderate.

467 Bearing in mind the overall status and vulnerability conjointly, we can say that the
468 aquifer affected in the Plana de Oropesa-Torreblanca (47.6 – 86.7%) is similar to the
469 aquifer classified as vulnerable (56.6 – 99.8%) for both thresholds. However, in the
470 Plana de Vinaroz, though the majority of the aquifer is vulnerable (94.1% with an index
471 of moderate vulnerability), not all of it exhibits SWI problems (the aquifer affected by
472 high chloride concentration is less than 66% of the total aquifer).

473

474 **Acknowledgments:** This work has been partially supported by the CGL2013-48424-
475 C2-2-R project and the Plan de Garantía Juvenil from Mineco, co-financing by BEI and
476 FSE.

477

478 **REFERENCES:**

479 Aller L, Bennett T, Lehr JH, Perry RJ, Hackett G (1987) DRASTIC: a standardized
480 system for evaluating groundwater pollution potentials using hydrogeological settings.
481 Environmental Protection Agency, EPA 600/2-87-035; pp 622

482

483 Arslan H, Cemek B, Demir Y (2012) Determination of seawater intrusion via
484 hydrochemicals and isotopes in Bafra plain, Turkey. *Water Resour Manag*
485 26(13):3907–3922. doi:10.1007/s11269-012-0112-3

486

487 Ballesteros BJ, Morell I, García-Menéndez O, Renau-Pruñonosa A (2016) A
488 Standardized Index for Assessing Seawater Intrusion in Coastal Aquifers: The SITE
489 Index. *Water Resour Manag* 30(13): 4513-4527. doi: 10.1007/s11269-016-1433-4

490

491 Barlow PM, Reichard EG (2010) Saltwater intrusion in coastal regions of North
492 America. *Hydrogeol J* 18 (1):247–260 <https://doi.org/10.1007/s10040-009-0514-3>

493

494 Barrocu G (2003) Seawater intrusion in coastal aquifers in Italy. *Coastal Aquifers*
495 *Intrusion Technology: Mediterranean Countries*. IGME (ed). ISBN:84-7840-470-8

496

497 Benini L, Antonellini M, Laghi L (2016) Assessment of water resources availability and
498 groundwater salinization in future climate and land use change scenarios: A case study
499 from a coastal drainage basin in Italy. *Water Resour Manag* 30:731–745.
500 doi:10.1007/s11269-015-1187-4

501

502 Boschetti T, González-Hernández P, Hernández-Díaz R, Naclerio G, Celico F (2015)
503 Seawater intrusion in the Guanahacabibes Peninsula (Pinar del Río Province, western
504 Cuba): effects on karst development and water isotope composition. *Environ Earth Sci*
505 73:5703–5719. doi:10.1007/s12665-014-3825-1
506
507 Bouderbala A (2015) Groundwater salinization in semi-arid zones: an example from
508 Nador plain (Tipaza, Algeria). *Environ Earth Sci* 73:5479–5496. doi:10.1007/s12665-
509 014-3801-9
510
511 Chachadi AG, Lobo-Ferreira JP. (2001) Sea water intrusion vulnerability mapping of
512 aquifers using GALDIT method. In: Proc. Workshop on Modelling in Hydrogeology
513 (Anna University, Chennai), 143–156, and in COASTIN A Coastal Policy Research
514 Newsletter, Number 4, March 2001. New Delhi, TERI, 7–9, (cf. [http://www.teriin.org/-](http://www.teriin.org/-teri-wr/coastin/newslett/coastin4.pdf)
515 [teri-wr/coastin/newslett/coastin4.pdf](http://www.teriin.org/-teri-wr/coastin/newslett/coastin4.pdf))
516
517 Chachadi AG, Lobo-Ferreira JP (2005) Assessing aquifer vulnerability to sea-water
518 intrusion using GALDIT method: part 2 – GALDIT indicator descriptions. IAHS and
519 LNEC, Proceedings of the 4th The Fourth Inter Celtic Colloquium on Hydrology and
520 Management of Water Resources, held at Universidade do Minho, Guimarães, Portugal,
521 July 11–13, 2005
522
523 CHJ (2016) (Júcar Water Agency) Júcar River Basin Plan. Demarcación hidrográfica
524 del Júcar. Confederación Hidrográfica del Júcar. Ministry of Agriculture, Food and
525 Environment, Spain
526

527 Civita M.V (1994). Le carte della vulnerabilità degli acquiferi all'inquinamento: Teoria
528 & pratica (Groundwater Vulnerability Maps to Contamination: Theory and Practice).
529 Pitagora, Bologna
530

531 Custodio E (2010) Coastal aquifers of Europe: an overview. *Hydrogeol J* 18:269–280
532

533 Doerfliger N, Jeannin PY, Zwahlen F (1999) Water vulnerability assessment in karst
534 environments: a new method of defining protection areas using a multi-attribute
535 approach and GIS tools (EPIK method). *Environ Geol* 39:165–176
536

537 Dahlstrom K, Müller D (2006) D14: Report on National Methodologies for
538 Groundwater Threshold Values. BRIDGE project, Background Criteria for the
539 Identification of Groundwater Thresholds, 6th Framework Programme Contract, 6538
540

541 Eeman S, Leijnse A, Raats PAC, Van Der Zee SEATM (2011) Analysis of the thickness
542 of a fresh water lens and of the transition zone between this lens and upwelling saline
543 water. *Adv Water Resour* 34:291–302. doi:10. 1016/j.advwatres.2010.12.001
544

545 García-Menéndez O, Morell I, Ballesteros BJ, Renau-Pruñonosa A, Esteller MV (2016)
546 Spatial characterization of the seawater upconing process in a coastal Mediterranean
547 aquifer (Plana de Castellón, Spain): evolution and controls. *Environ Earth Sci* 75:728.
548 doi:10.1007/s12665-016-5531-7
549

550 Guhl F, Pulido-Bosch A, Pulido-Leboeuf P, Gisbert J, Sánchez-Martos F, Vallejos A
551 (2006) Geometry and dynamics of the freshwater-seawater interface in a coastal aquifer
552 in southeastern Spain. *Hydrolog Sci J* 51(3): 543–555. doi:10.1623/hysj.51.3.543
553

554 Günay G (1997) Solutions of seawater intrusion problems in Turkey. Chap. 15 of
555 Seawater intrusion in coastal aquifers. Guidelines for study, monitoring and control.
556 FAO. 153 pp. ISBN:92-5-103986-0
557

558 Kazakis N, Pavlou A, Vargemezis G, Voudouris KS, Soulios G, Pliakas F, Tsokas G
559 (2016) Seawater intrusion mapping using electrical resistivity tomography and
560 hydrochemical data. An application in the coastal area of eastern Thermaikos Gulf,
561 Greece. *Sci Total Environ* 543:373–387. doi:10.1016/j.scitotenv.2015.11.041
562

563 Kumar P, Bansod BK, Debnath SK, Thakur PK, Ghanshyam C (2015) Index-based
564 groundwater vulnerability mapping models using hydrogeological settings: a critical
565 evaluation. *Environmental Impact Assessment Review* 51: 38-49
566

567 Llopis-Albert C, Pulido-Velazquez D (2014) Discussion about the validity of sharp-
568 interface models to deal with seawater intrusion in coastal aquifers. *Hydrol Process*
569 28:3642–3654. doi:10.1002/hyp.9908
570

571 Parck Y, Lee JY, Kim JH, Song SH (2012) National scale evaluation of groundwater
572 chemistry in Korea coastal aquifers: evidences of seawater intrusion. *Environ Earth Sci*
573 66:707–718. doi:10.1007/s12665-011-1278-3
574

575 Petalas C, Lambrakis N (2006) Simulation of intense salinization phenomena in coastal
576 aquifers of Thrace. *J Hydrol* 324:51–64. doi:10.1016/j.hydrol.2005.09.031
577

578 Pratheepa V, Ramesh S, Sukumaran N, Murugesan AG (2015) Identification of the
579 sources for groundwater salinization in the coastal aquifers of Southern Tamil Nadu,
580 India. *Environ Earth Sci* 74:2819–2829. doi:10.1007/s12665-015-4303-0
581

582 Renau Pruñonosa, A (2013) Nueva herramienta para la gestión de las aguas
583 subterráneas en acuíferos costeros. Volumen ecológico de remediación (VER).
584 Metodología y aplicación a la Plana de Oropesa-Torreblanca (MASub 080.110),
585 Universitat Jaume I
586

587 Smith AJ (2004) Mixed convection and density-dependent seawater circulation in
588 coastal aquifers. *Water Resources Research* 40: W083091-W.083091. doi:
589 10.1029/2003WR002977
590

591 Stempvoort DV, Ewert L, Wassenaar L (1993) Aquifer vulnerability index: a GIS-
592 compatible method for groundwater vulnerability mapping. *Canadian Water Resources*
593 *Journal*, 18: 25-37
594

595 Steyl G, Dennis I (2010) Review of coastal-area aquifers in Africa. *Hydrogeol J*
596 18:217–225. doi:10.1007/s10040-009-0545 9
597

598 Trabelsi N, Triki I, Hentati I, Zairi M (2016) Aquifer vulnerability and seawater
599 intrusion risk using GALDIT, GQISWI and GIS: case of a coastal aquifer in Tunisia.
600 *Environmental Earth Sciences*, 75: 1-19
601

602 Water Framework Directive (WFD 2000) Directiva 2000/60/CE del Parlamento
603 Europeo y del Consejo de 23 de Octubre de 2000. Diario Oficial de las Comunidades
604 Europeas de 22/12/2000. L 327/ 1–327/32
605

606 Werner AD, Gallagher MR (2006) Characterisation of sea-water intrusion in the Pioneer
607 Valley, Australia using hydrochemistry and three-dimensional numerical modelling.
608 *Hydrogeol J* 14:1452–1469
609

610 Werner AD, Ward JD, Morgan LK, Simmons CT, Robinson NI, Teubner MD (2012).
611 Vulnerability indicators of sea water intrusion. *Ground Water*, 50(1), 48-58
612

613 Wriedt G, Bouraoui F (2009) Large scale screening of seawater intrusion risk in Europe
614 – methodological development and pilot application along the Spanish Mediterranean
615 coast. Luxembourg: European Commission, Joint Research Centre, Institute for
616 Environment and Sustainability. doi.org/10.2788/19371

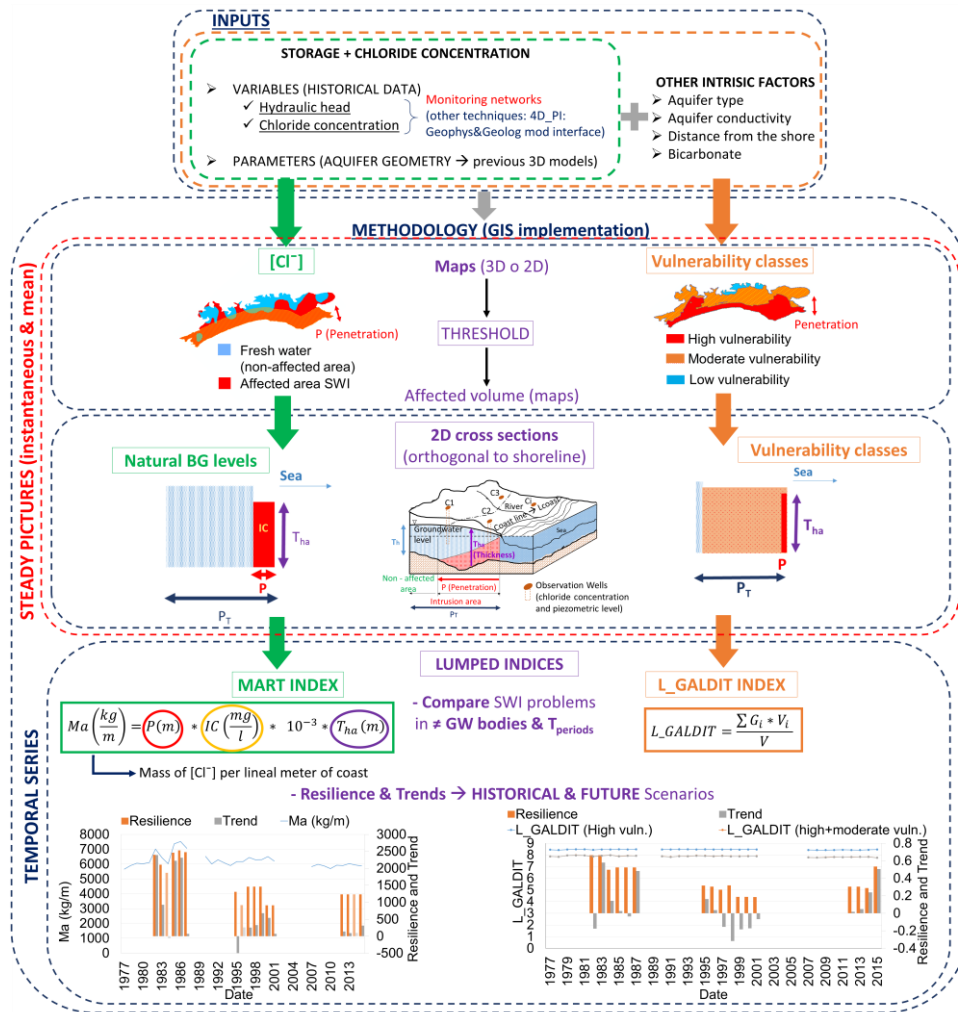


Fig 1 Flow chart of methodology

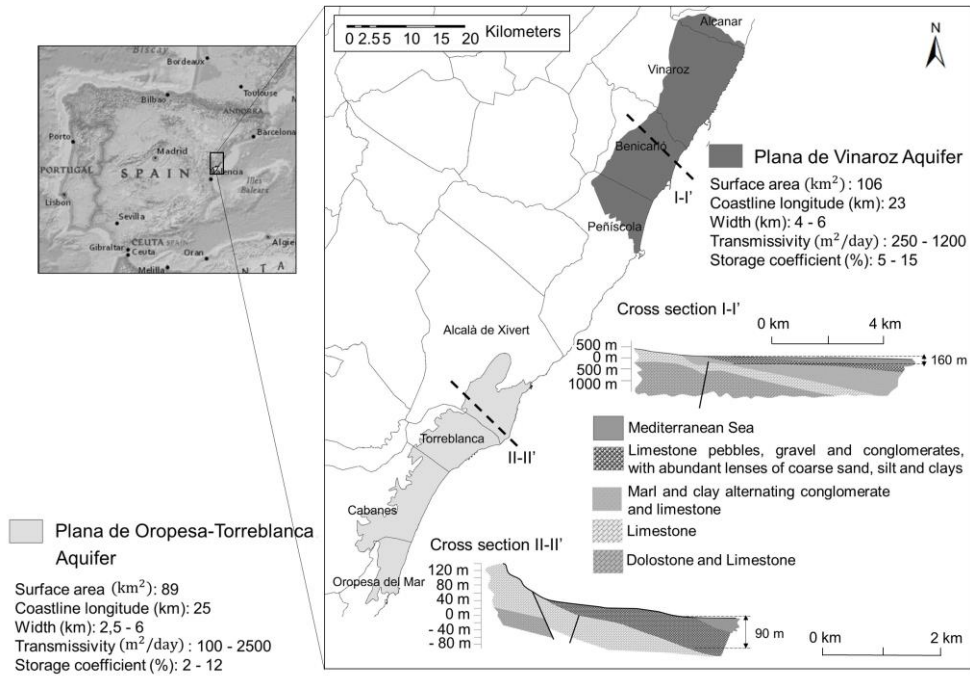


Fig 2 Situation of the study area and hydrogeology

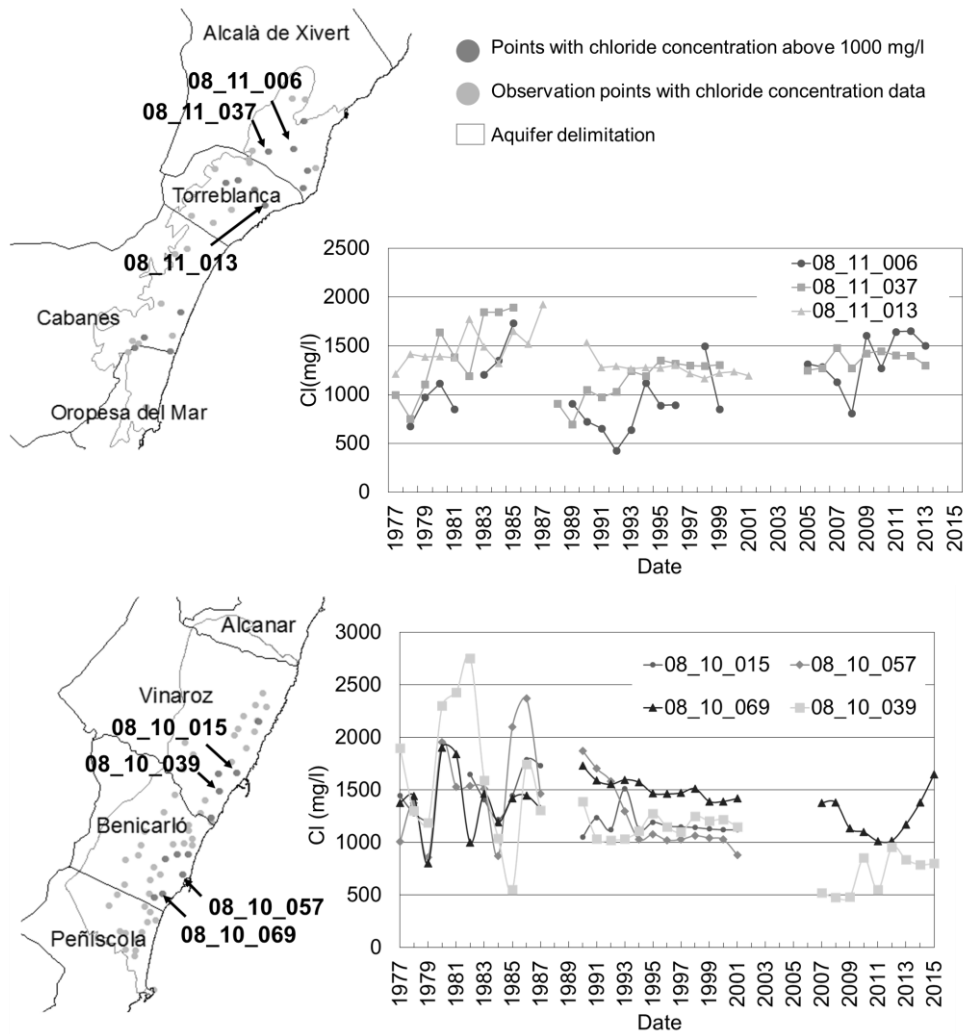


Fig 3 Observation points for chloride concentration and evolution of the chloride concentrations in monitoring points in Plana de Oropesa-Torreblanca (top) and Plana de Vinaroz (down) aquifers

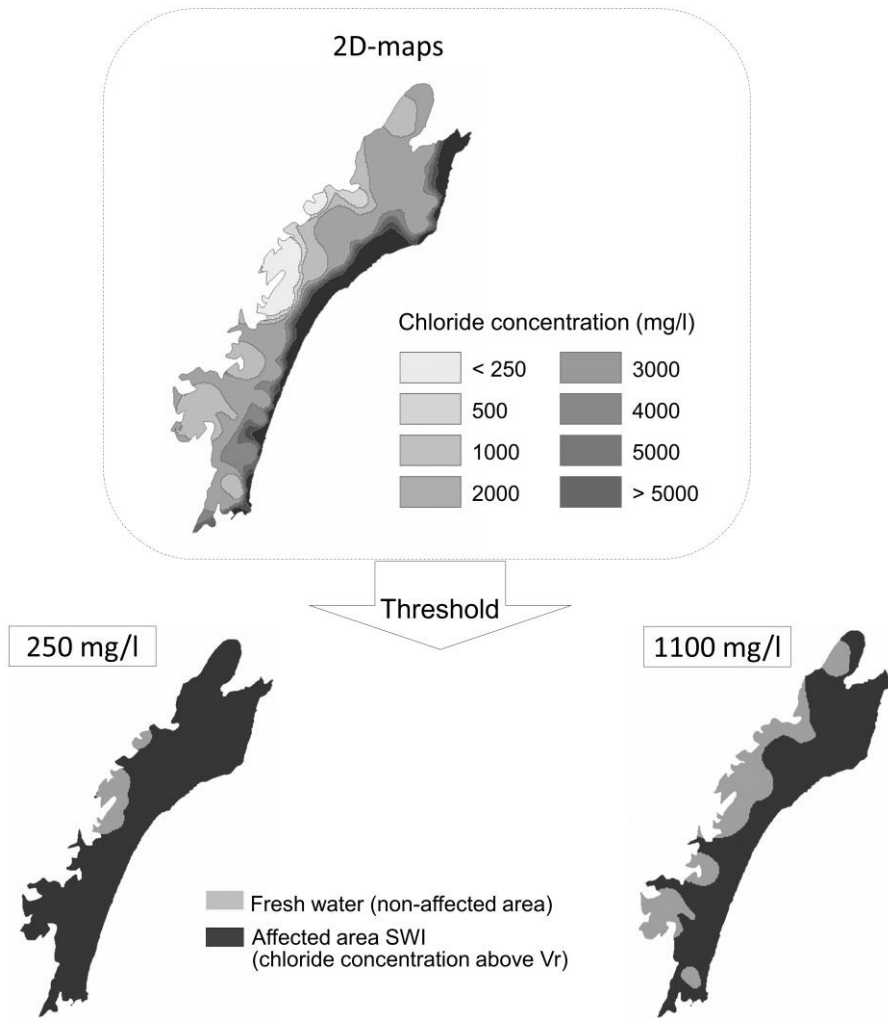


Fig 4 Chloride concentration maps in Plana de Oropesa-Torreblanca for October 1985

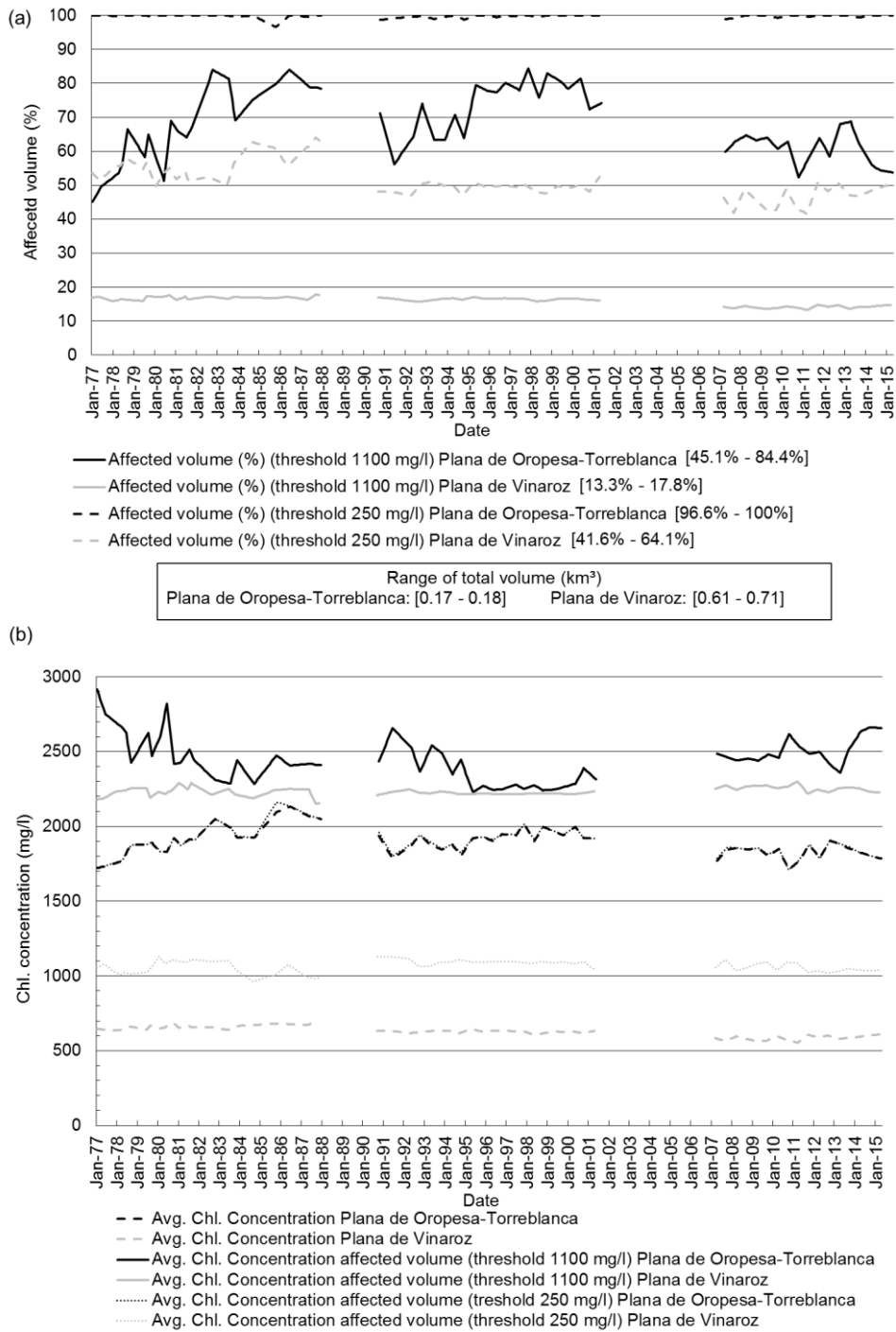


Fig 5 Evolution of (a) affected volume (rg (%)) and (b) average chloride concentration in total aquifer and in the affected volume for the two aquifers

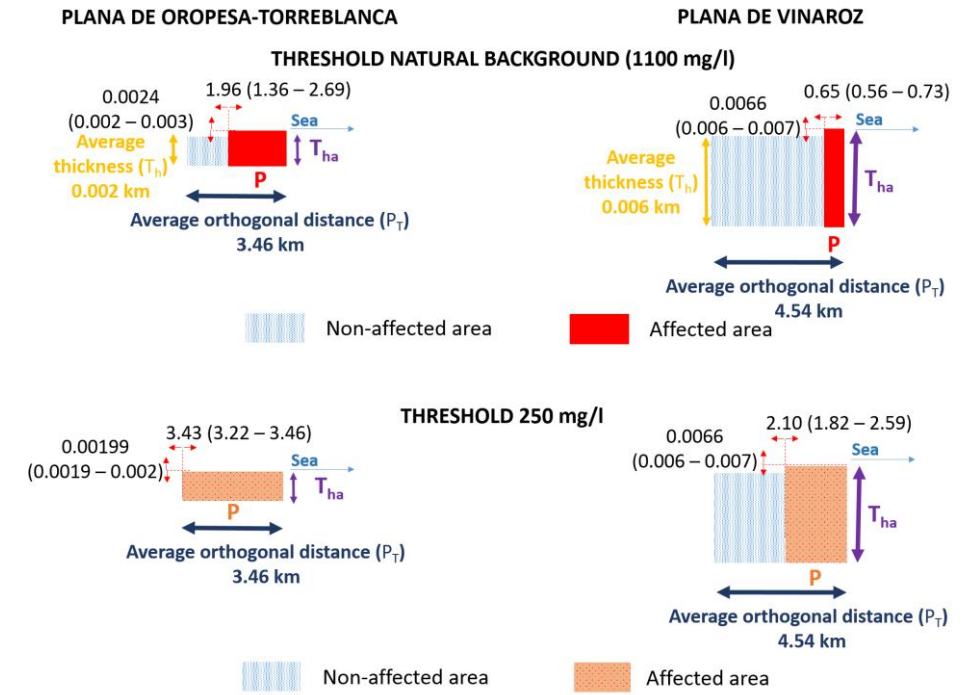


Fig 6 Average cross-sections for two thresholds (natural background and 250 mg/l) (MART index) over the period 1977-2015 (vertical exaggeration scale: 500)

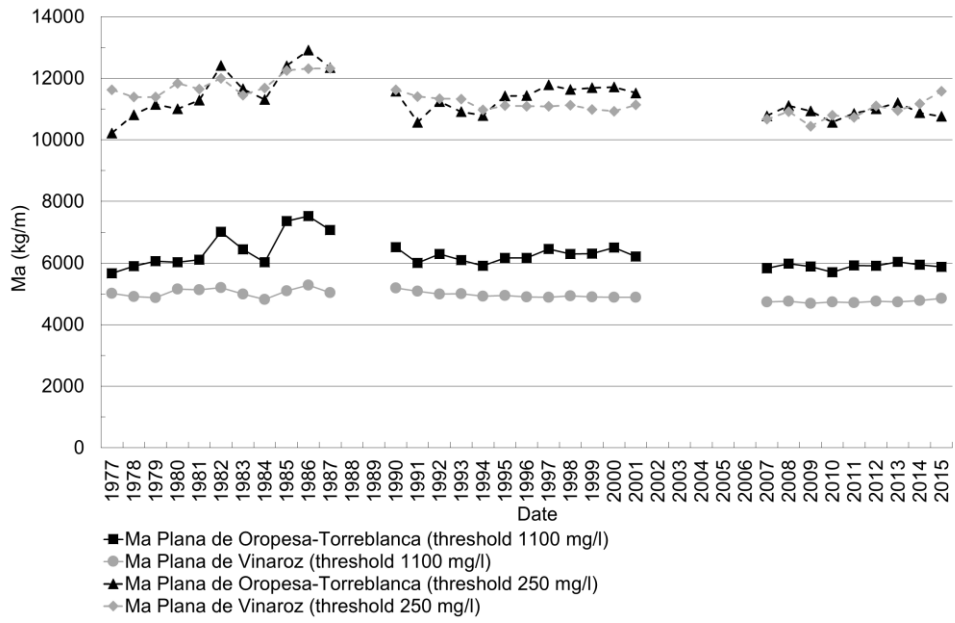


Fig 7 Evolution of the global index, Ma, in the two aquifers studied

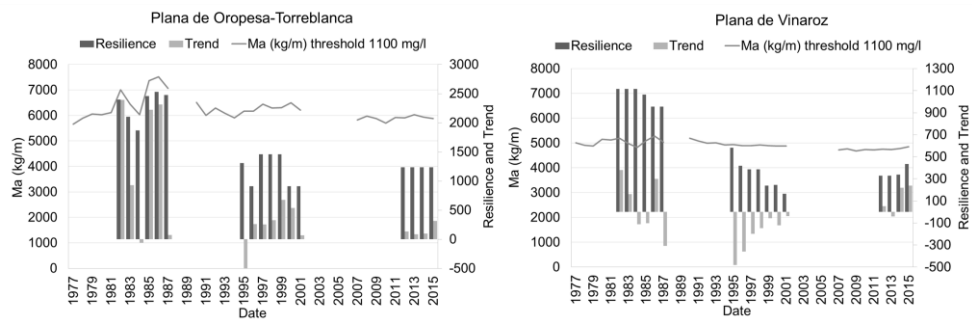


Fig 8 Ma, Resilience and Trend in Plana de Oropesa-Torreblanca and Plana de Vinaroz aquifers (scale exaggeration Resilience and Trend: 10000)

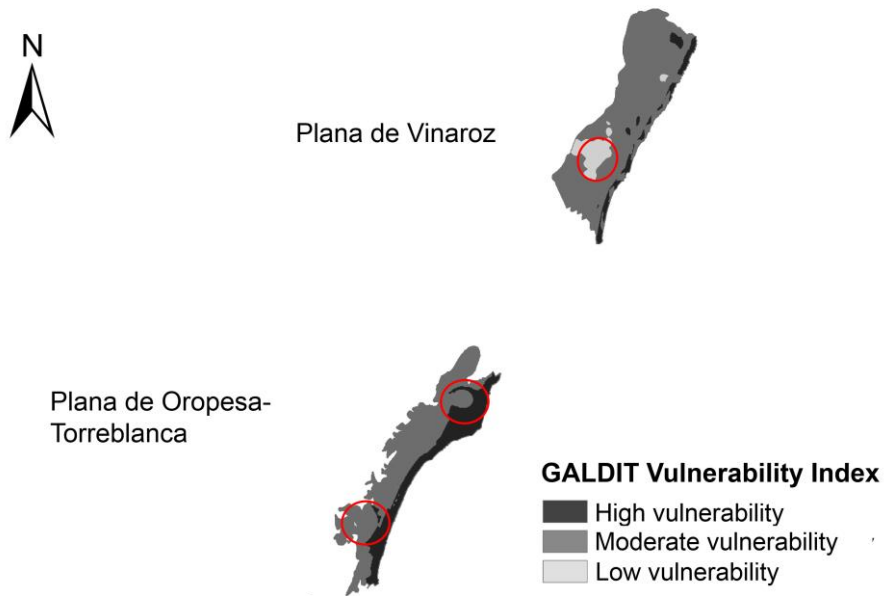


Fig 9 L_GALDIT maps in Plana de Oropesa-Torreblanca for April 2015

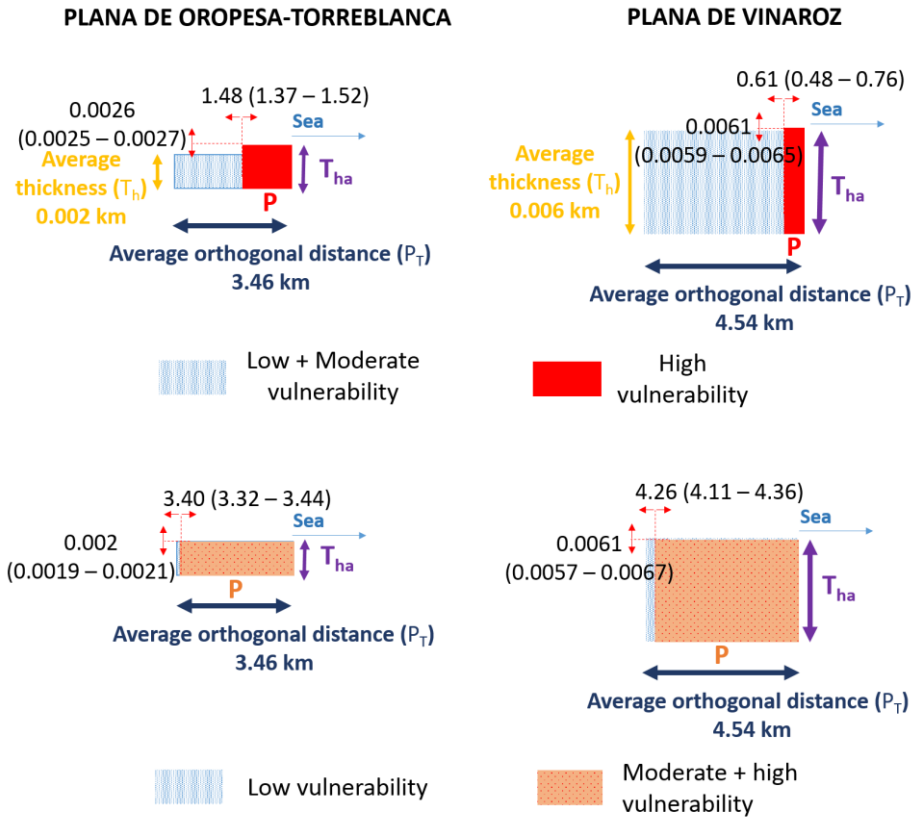


Fig 10 Average cross-sections in two aquifers (L_GALDIT index) for the period 1977-2015 (vertical exaggeration scale: 500)

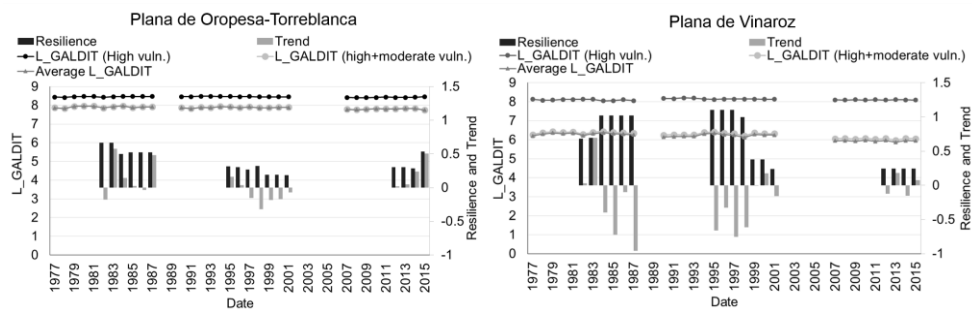


Fig 11 L_GALDIT, Resilience and Trend in Plana de Oropesa-Torreblanca and Plana de Vinaroz aquifers (scale exaggeration Resilience and Trend: 100)